# **Mechanical Pulping**

Christer Sandberg, Stefan B. Lindström, Kateryna Liubytska and Fritjof Nilsson\*

# Development of handsheet mechanical properties linked to fibre distributions in two-stage low consistency refining of high yield pulp

https://doi.org/10.1515/npprj-2024-0083 Received November 20, 2024; accepted January 16, 2025; published online February 17, 2025

**Abstract:** In this study, a two-stage, low-consistency (LC) refining process at the Holmen Braviken paper mill in Sweden was examined to evaluate the relationship between energy input, fibre distributions, and pulp properties, including handsheet properties. The LC refiners used thermo-mechanical pulp based on 100 % Norway spruce, with two specific energy levels: "low" (≈80 kWh/adt) or "high" (≈100 kWh/adt). All four permutations of these settings were examined. Overall, higher refining efficiency (measured by the increase in tensile index per applied energy) was observed in the first LC refiner stage than in the second. To further explore the impact of LC refining, pulp particle distributions were investigated. Samples from before, between and after the two LC stages were analysed using an optical fibre analyser, which provided detailed data on length-width-curl-fibrillation distributions. The impact of LC refining on these distributions was quantified using Kolmogorov-Smirnov statistics, highlighting statistically significant changes observed in the length and curl distributions. We investigated the correlation between energy input into the LC refiners and the impact on fibre distributions and handsheet properties. These insights underscore the effectiveness of our analytical approach and its potential for refining process control in mechanical pulping, offering a method for more targeted and efficient adjustments.

**Keywords:** LC refining; energy efficiency; fibre distribution; TMP; mechanical pulp

**Stefan B. Lindström and Kateryna Liubytska**, FSCN Research Centre, Mid Sweden University, 851 70 Sundsvall, Sweden

# 1 Introduction

Low consistency (LC) refining is widely applied in mechanical and chemimechanical pulping for the development of fibre properties. It can be applied in different positions in a mechanical pulping process which, to some extent, affects fibre development and refining efficiency, defined as tensile index increment per applied specific energy (Sandberg et al. 2017). From the mid-1990s, LC installations in thermomechanical pulp (TMP) lines were often as third stage mainline refiners (e.g. Musselman et al. 1997) and in modern chemithermomechanical pulp (CTMP) lines both in the main- and reject lines (e.g. Peng et al. 2018). Earlier studies have shown that fibre properties are not developed in the same way in LC refining as in high consistency (HC) refining (Andersson et al. 2012; Ferritsius et al. 2012, 2020; Gorski et al. 2012). The fibres are subjected to less peeling in LC than in HC refining, resulting in fewer fines being generated. LC refining seems to produce more internal than external fibrillation, however the increase in internal fibrillation is not more efficient than for high intensity HC refining (Fernando et al. 2013; Ferritsius et al. 2020; Gorski et al. 2012). This could be one reason for the comparatively lower increase in light scattering coefficient across LC refiners. Another distinct difference is that fibres are straightened during LC refining, whereas they either maintain their original shape or become more curled during HC refining. However, the underlying reason for this disparate development is not well understood.

When multiple LC refiners are incorporated into a TMP line, they are often installed in parallel, which enables convenient adaptation to the production rate in the pulp line. However, it is also possible to arrange the refiners in series, a configuration that is more common in the processing of softwood kraft pulp but also in modern CTMP mills (e.g. Guangdong et al. 2011). Two-stage LC refining was shown to be beneficial for refining of high-freeness groundwood, as higher tensile index was attained at a given freeness than for single-stage refining (Montmorency 1958). LC refining of TMP in two or more stages in series has been studied in pilot trials

<sup>\*</sup>Corresponding author: Fritjof Nilsson, FSCN Research Centre, Mid Sweden University, 851 70 Sundsvall, Sweden; and Department of Fibre and Polymer Technology, School of Chemical Science and Engineering, KTH Royal Institute of Technology, SE-100 44 Stockholm, Sweden, E-mail: fritjofn@kth.se. https://orcid.org/0000-0002-5010-5391
Christer Sandberg, Holmen AB, 601 88 Norrköping, Sweden, E-mail: christer.sandberg@holmen.com

(see e.g. Gorski et al. 2012; Sabourin 2007). However, those studies, and other earlier investigations, have not focused the fibre development of each stage in detail. Moreover, the refining efficiency, defined as the tensile index increase per MWh/ton, for LC refiners in a two-stage process, is lower for the second stage than the primary stage (Sandberg et al. 2021). The reason for this difference is yet to be understood.

The objective of this study was to examine how fibre property distributions measured with an optical fibre analyzer and handsheet properties are affected by changing the specific refining energy in a two-stage LC refining process. A combination of handsheet characterization, optical fibre analysis, and fibre distribution analysis using Kolmogorov-Smirnoff statistic and two-dimensional (2D) visualization techniques was used to achieve this.

# 2 Theory

In this work, we take interest in comparing different pulp particle distributions to identify statistically significant differences between them, and to quantify these differences. The purpose is to relate changes in the distributions to changes in handsheet mechanical properties. We base the test statistic on empirical cumulative distribution functions.

For a sample  $A = X_1, X_2, ..., X_{n_A}$  of size  $n_A$ , we define its empirical distribution function as

$$\tilde{\Phi}_{A}(x) = \frac{1}{n_{A}} \sum_{i=1}^{n_{A}} I(x \ge X_{i}),$$
(1)

where  $I(\cdot)$  is the indicator function, and a superposed tilde indicates an empirical distribution. The empirical distribution function is a lossless representation of A; the observations in *A* can be recovered from  $\tilde{\Phi}_A(x)$ .

Consider two samples, A and B, with sizes  $n_A$  and  $n_B$ , respectively. The samples are drawn from the continuous cumulative distribution functions  $\Phi_A(x)$  and  $\Phi_B(x)$ . The null hypothesis is:

$$H_0: \Phi_A(x) = \Phi_B(x). \tag{2}$$

The purpose of a two-sample test is to investigate whether  $H_0$  can be rejected at a given level of significance  $\alpha \in$ (0, 1) based on the samples A and B. Many two-sample statistical tests have been proposed based on the difference (Anderson and Darling 1952; Cramer 1928; Kolmogorov 1933; Kuiper 1960; Smirnov 1944; von Mises 1928),

$$D_{AB}(x) = \tilde{\Phi}_B(x) - \tilde{\Phi}_A(x). \tag{3}$$

Particularly, the one-dimensional, two-sample Kolmogorov-Smirnov (KS) test (Kolmogorov 1933; Smirnov 1944) rejects  $H_0$  at significance  $\alpha$  if (Stephens 1970)

$$p_{\text{KS}}\left(\left[\sqrt{n_{\text{e}}} + 0.12 + \frac{0.11}{\sqrt{n_{\text{e}}}}\right] \sup_{x \in \mathbb{R}} |D_{AB}(x)|\right) < \alpha, \tag{4}$$

where  $n_e = n_A n_B / (n_A + n_B)$  is the effective number of samples, while the function for calculating the p-value is (Marsaglia et al. 2003):

$$p_{KS}(\lambda) = 2\sum_{j=1}^{\infty} (-1)^{j-1} e^{-2j^2 \lambda^2}.$$
 (5)

Equation (4) is suitable for comparing pulp samples before and after LC refiner steps, or indeed any unit process. In addition, since fibre data from n = 6 to n = 12 beakers of diluted pulp suspension are combined in each measurement, Equation (4) can also test whether the content of any of the beakers is significantly different than the other beakers within the same pulp sample. This can either be performed by comparing each beaker with a collective sample of all other beakers, or by comparing all pairs of beakers. When comparing several samples, the significance level  $\alpha$  should however be adjusted using Bonferroni correction, such that the adjusted significance level becomes  $\alpha^* = \alpha/N$ , where *N* is the number of independent comparisons. The default value of  $\alpha$  is 0.05 in this work.

As an alternative to Equation (4), since  $p_{KS}:[0,\infty)\to$ [0,1) is invertible, we can introduce a scaled distribution difference,

$$D_{AB}^{*}(X;\alpha) = \frac{\sqrt{n_{\rm e}} + 0.12 + \frac{0.11}{\sqrt{n_{\rm e}}}}{p_{\nu_{\rm c}}^{-1}(\alpha)} D_{AB}(X), \tag{6}$$

which permits us to formulate the two-sample KS test as

$$\sup_{\mathbf{x} \in \mathbb{D}} \left| D_{AB}^* \left( \mathbf{x} \; ; \; \alpha \right) \right| > 1. \tag{7}$$

Our introduction (6) of  $D_{AB}^*(x;\alpha)$  serves a multifaceted role. Besides its extremal values signalling significant distributional discrepancies through the KS test, we aim herein to explore how it can be used as a more comprehensive metric for qualitative and quantitative distributional differences.

As a demonstration, we consider two different lognormal distributions whose probability density functions,  $\phi_A(x)$  and  $\phi_B(x)$ , are illustrated in Figure 1a. When samples A and B are drawn from these distributions, we obtain empirical CDFs (Figure 1b). Finally, the scaled difference  $D_{AB}^*(x;\alpha)$  is plotted in Figure 1c. It shows a peak located at  $x \approx 3$ , which is also where the PDFs intersect. The fact that  $\max_{x} |D_{AB}^{*}(x)| > 1$ means that the difference between the empirical CDFs is significant. A positive peak in  $D_{AB}^*(x;\alpha)$  corresponds to an overall reduction of the observable x in B compared to A. Particularly, the frequency has decreased in the interval

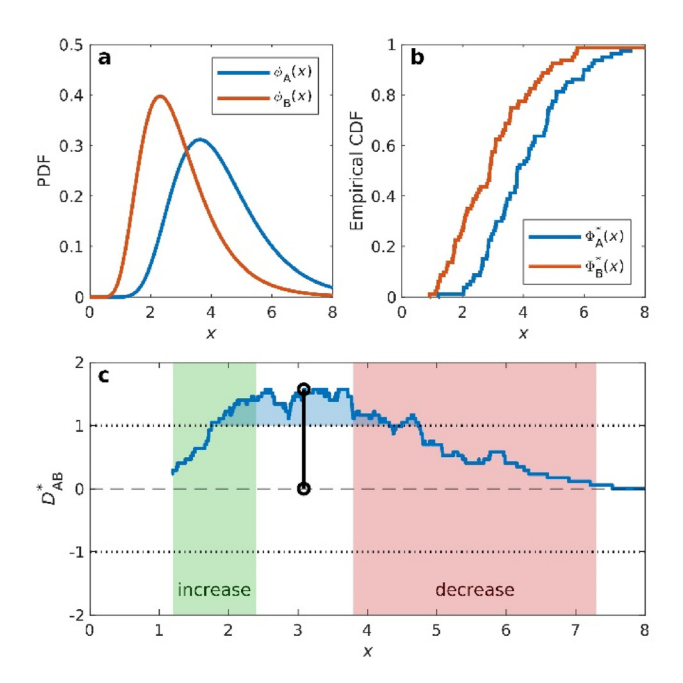


**Figure 1:** A demonstration of how two distributions can be compared. (a) PDFs for two different lognormal distributions. (b) Empirical CDFs for samples, each one of size 100, drawn from the two different lognormal distributions. (c) Scaled difference between empirical PDFs. The dotted lines indicate a difference at significance level  $\alpha = 0.05$ . A positive slope of  $D^*_{AB}$  indicates that frequency is increasing in B as compared to A within that interval. The opposite holds true for a negative slope.

where  $D_{AB}^*(x;\alpha)$  exhibits a negative slope, while it has increased in the interval with positive slope.

# 3 Materials and methods

A two-stage LC refining process in the Holmen Braviken mill in Sweden was studied. The LC refiners (TwinFlo 52, Andritz) were fed with TMP based on 100 % Norway spruce from a two-stage HC refiner line (Twin 60, Andritz). Pulp samples were taken at the positions marked with red crosses in Figure 2.

The pulp consistency was 4.5%, the flow through the refiners was 104–108 l/s and the production rate was around 17 bdt/h. The feed pulp temperature was around 77 °C during the trial. Both refiners were equipped with Valmet segments:

Figure 2: The studied TMP line in Braviken with two-stage LC refining.

Primary – SWPS258F37/M37 on the rotor and SWP5258E72/M72 on stators. Secondary – SWP5258D61/M61 on both rotor and stators. The coarser segment design in the first stage is used to avoid plugging by pin-chips which occasionally are created during startup of the TMP line.

For each LC refiner, the load was set at either "low" ( $\approx$ 80 kWh/bdt) or "high" ( $\approx$ 100 kWh/bdt), based on the typical operating range in mill installations, where good refining efficiency is achieved without excessive fiber length reduction. The specific refining energy was calculated from the gross motor power, including the no-load (idle) power. Pulp samples were collected for all four permutations of the Low and High settings, as shown in Table 1.

All samples were hot disintegrated according to (ISO 5263-3:2004) before analysis. Canadian standard freeness (CSF) was measured according to (ISO 5267-2:2001).

Handsheets were made according to ISO 5269-1:2005 without white water recirculation. The following measurements were made on handsheets: apparent density (ISO 534), tensile index (ISO 1924-2), light scattering coefficient, 550 nm, (ISO 9416), burst index (ISO 2758), and SCT index (ISO 9895). Each tensile index measurement was made on an increased number of 16 strips.

Pulp samples were analysed in a L&W Fiber Tester plus from ABB. The analyser assigns each detected particle five attributes: fibre length L, width W, shape factor S (i.e. end-to-end length divided by contour length), perimeter-based fibrillation, and area-based fibrillation. The curl index, C, is calculable from the shape factor (Page et al. 1985). Each data point was based on measurements from 6 to 12 beakers of diluted pulp suspension. The particle size constraint was set to  $L \geq 0.2$  mm, resulting in an average of approximately 80,000 particles analyzed for each data point.

# 4 Results

### 4.1 Energy efficiency

The energy split between the two LC refining stages (Low-High or High-Low) did not affect the tensile index increase in any systematic way, Figure 3. However, on average, the tensile index increase was larger for the first stage than for the second stage. The average refining efficiency (or the slope in Figure 3) for the primary LC refining stage was 38 (Nm/g)/(MWh/bdt) and 24 (Nm/g)/(MWh/bdt) for the second LC refining stage. In Figure 3, recalculated data from Sabourin (2007) are also shown. The points represent three sequential

**Table 1:** Process settings for the two LC refiners.

		Tri	al 1	Trial 2		Tri	al 3	Trial 4		
		Low-Low		High-Low		Low	-High	High-High		
		LC1	LC2	LC1	LC2	LC1	LC2	LC1	LC2	
Gross power	MW	1.38	1.37	1.72	1.4	1.39	1.71	1.69	1.67	
Flow	l/s	101	103	101	102	101	104	101	102	
SRE, gross	kWh/bdt	84	82	105	85	85	101	103	101	
SEL	J/m	0.99	0.63	1.33	0.65	1	0.86	1.3	0.83	

LC refining stages of white spruce in a pilot refiner. Sabourin's investigation similarly indicates a decrease in refining efficiency for each stage, although Sabourin neither commented on this trend nor showed any detailed data from each refining stage. The refining efficiency of the pilot data is higher compared to the present study, but it is not clear from Sabourin's work whether the presented specific refining energy (SRE) was net or gross, *i.e.* whether the no-load power was included or not. Most likely it is the net specific energy. In the present work, the no-load is included in the SRE. Additionally, differences in spruce species between the TMPs might influence the observed refining efficiencies.

The refining efficiency of the second LC refining stage is only slightly higher than the 20 (Nm/g)/(MWh/adt) reported by Hill et al. (2017) and Sandberg et al. (2017) for second stage

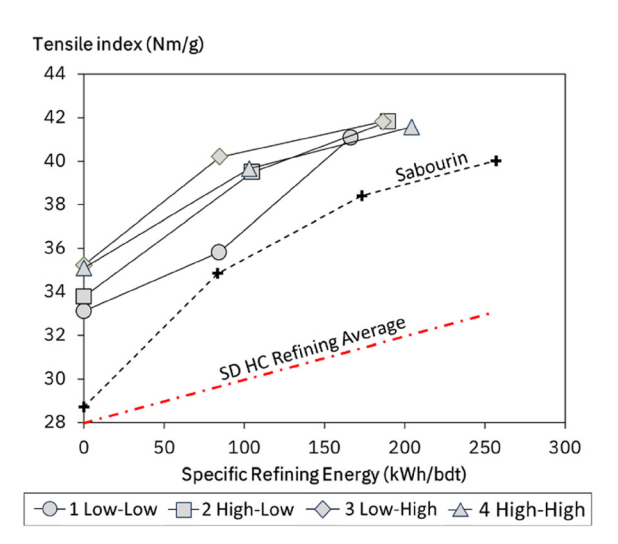


**Figure 3:** The average tensile index increase is larger for the first LC refining stage than for the second stage. Data from three consecutive LC refining stages are also shown, recalculated from Sabourin (2007). A line showing average tensile index increase for second stage single disc HC refining is included for comparison.

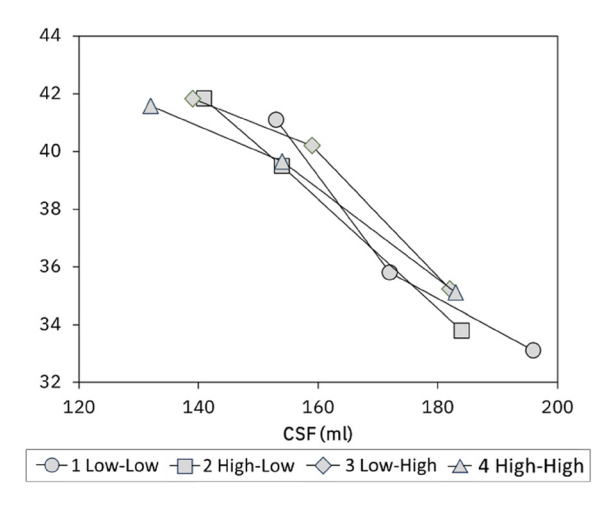
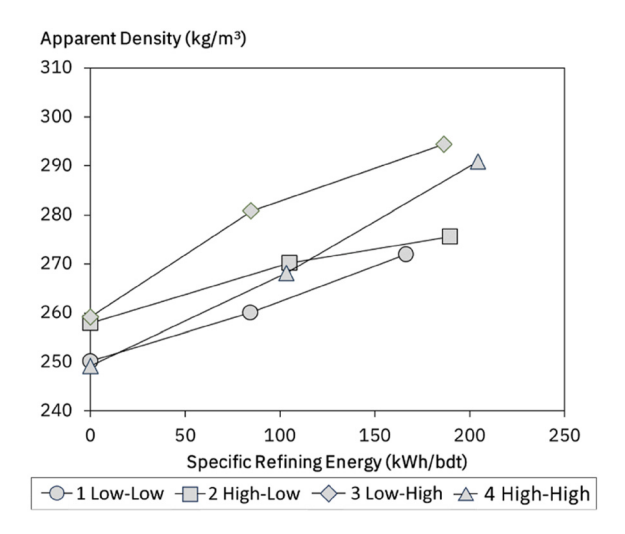


Figure 4: Tensile index versus CSF.

single disc (SD) HC refining. The average total refining efficiency of the two LC refiners was 31 (Nm/g)/(MWh/adt), which is higher than for SD HC refining, but it is interesting that the refining efficiency of the second LC refining stage is similar to HC refining. Why is it so?

In Figure 4, tensile index is shown as a function of freeness (CSF), where the minimum CSF observed in our trials is 132. The general trend is consistent with expectations; however, the tensile index after the first LC stage in the Low-Low series appears to be approximately 2 Nm/g higher than anticipated based on the overall trend. A similar deviation can also be observed in Figure 3 (tensile index vs. SRE), which suggests that this particular datapoint may be an outlier. This deviation could arise from measurement variability or differences in fiber properties after the first LC stage.

Other handsheet properties, *e.g.* apparent density (Figure 5), burst index (Figure 6) and strain at break (Appendix, Table A1) as well as length-length-weighted average fibre length (Figure 7) did not show a similar systematic trend with a lower change across the second-stage refiner.



**Figure 5:** Apparent density versus SRE did not show a lower slope for the second refining stage.

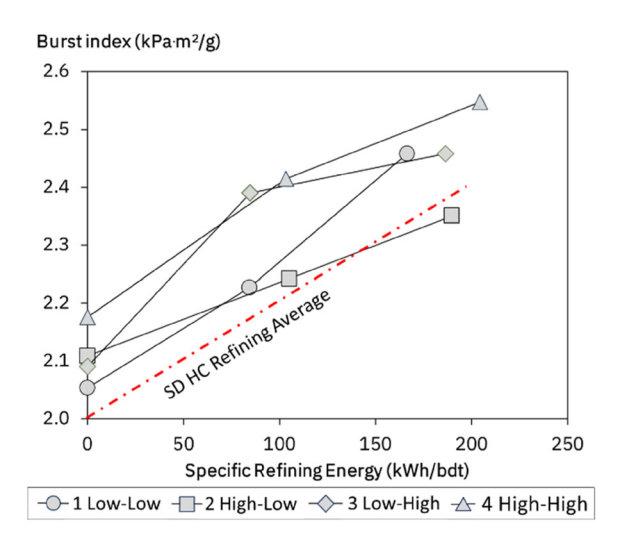


**Figure 6:** Burst index versus SRE did not show a distinctive lower slope for the second refining stage, and the increase is comparable to the average SD HC refining trend (dash-dotted line).

The data clearly shows that the most favourable mode of energy application in terms of fibre length at a given tensile index, is the Low-Low combination (Figure 8). The additional energy applied from Low-Low to High-High did not result in a significant increase in tensile index but a clear reduction in fibre length.

#### 4.2 Analysis with KS statistics

The pulps in the present study were further analysed using Kolmogorov-Smirnoff statistics, with the details of the four

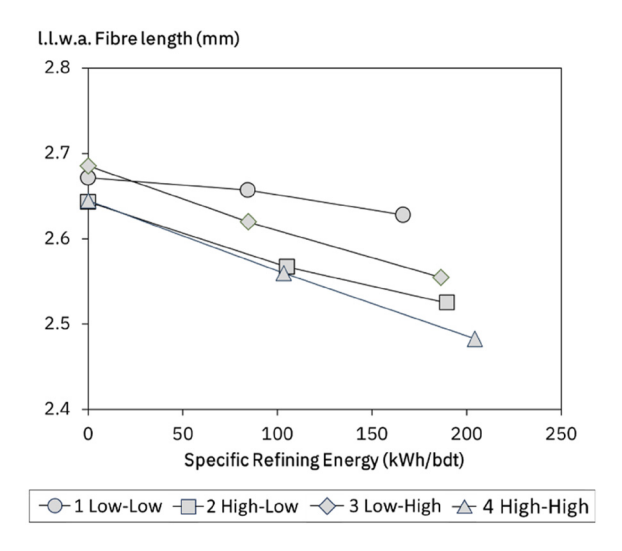


**Figure 7:** The two refining stages affected length-length-weighted average fibre length in a similar way. The trial with lowest specific energy in both stages had lowest overall reduction of fibre length.

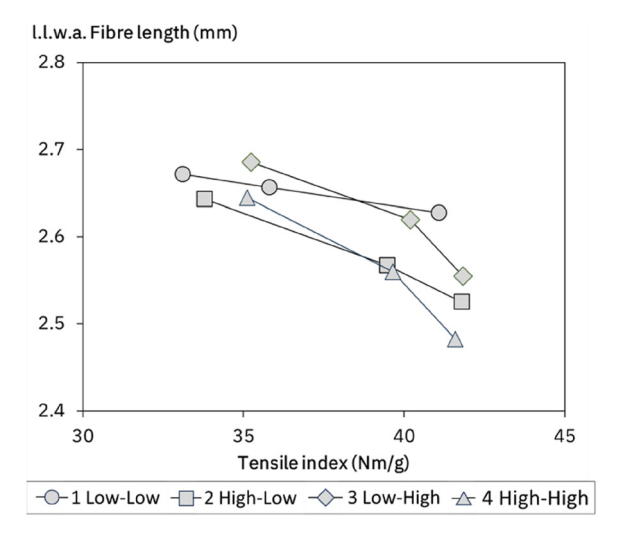


**Figure 8:** The Low-Low combination resulted in the highest fibre length at a given tensile index.

trials described in Table 1. Only pulp particles with  $L \ge 0.2$  mm were considered in the analysis, thus excluding the fines fraction. Moreover, we only present the distribution analysis for fibre length and curl index, since fibre width and fibrillation were less influenced by the LC refining according to our KS test (not shown). The work by Ferritsius et al. (2020) also shows that LC refining has a negligible effect on external fibrillation.

The KS analysis was performed in two steps: First a KS-test was applied to the individual beakers within each sample batch, to ensure that the subsamples were sufficiently

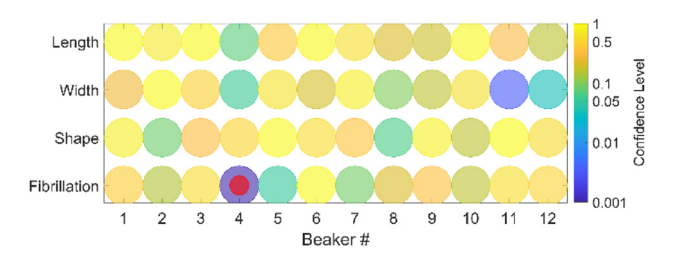


**Figure 9:** Typical KS probabilities when pairwise comparing 12 beakers with sub-samples from the same pulp with the other beakers. Darker colours indicate larger differences and red dots indicate that the samples are statistically different according to KS statistics.

similar. The outliers were removed and thereafter a second KS-test was applied to compare the effects of the four different trials.

In the first KS-test, a typical result when comparing each beaker from a batch to a collective sample of all other beakers from that same batch is shown in Figure 9. The beaker numbers are shown on the x-axes and the probability values from Equation (4) are shown as colours in the figure. Darker colours indicate lower p-values and thus larger differences between the particle distributions of the beakers. The number of independent comparisons is the product of the four properties multiplied with (n-1) comparisons per property, which is here N = 4(12-1) = 36. This gives an adjusted confidence level  $\alpha^* = \alpha/N = 0.05/36 = 0.0014$ . The perimeter-based fibrillation of beaker 4 deviates from the

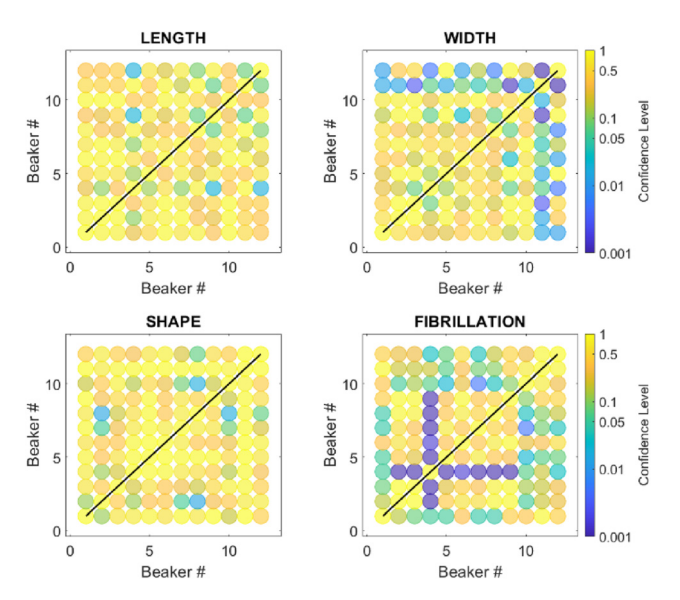


**Figure 10:** Typical KS probabilities when pairwise comparing 12 beakers with each other. The same beakers as in Figure 9 are analysed.

others in our example (Figure 9), but otherwise it cannot be refuted that particle distributions in different beakers are equal.

More detailed information about the differences between the beakers is obtained by also performing pairwise comparisons between each individual beaker in the batch (Figure 10). This complementary analysis shows that the fibrillation of beaker 4 deviates a lot from the other beakers. The width distributions of beakers 11 and 12 also differ a bit, but less than the adjusted confidence limit of Figure 9. A strict confidence level for the p-values in Figure 10 cannot be easily calculated, because some of the  $N = 4(n-1) \cdot n$  comparisons are dependent.

KS-analysis on individual beakers is useful for controlling samples prior to further analysis. For instance, Figures 9 and 10 indicate that beaker 4 should be excluded from that batch. When assessing corresponding data for all batches, the overall conclusion is that within each batch, the beakers typically exhibit statistically similar fibre distributions. Only a few exceptions were observed, and those beakers were excluded from subsequent analysis. Henceforth, a *sample* refers to the collective sample of all beakers from one batch, after data cleaning as described above.

The second KS-test was applied to compare the effects of different refining strategies. The four samples extracted before the primary LC stage are nominally the same, *i.e.* they were obtained at the same HC refiner settings. Since  $\max_L |D_{AB}^*(L)|$  exceeds 1 when comparing Trial 1 to each one of the other trials (Figure 11), the pulps were significantly different in Trial 1, even before LC refining. This deviation in fibre length distribution for Trial 1 is probably due to a temporary variation in the pulp quality from the preceding HC refiners (Figure 2).

We can compare the distributions of fibre lengths and curl index (Page et al. 1985) before and after each LC stage, remembering that peaks with positive sign indicate reduction of the average value. In each trial, 1 through 4, we observe that the first LC refining step has the greatest impact. In Figure 12, with data for Trial 1 (Low-Low), the magnitude of the  $D^*$  peaks are clearly higher across the first stage (LC1-Feed) than across the second stage (LC2-LC1). This holds true both for fibre length  $D^*_{AB}(L)$  and fibre curl  $D^*_{AB}(C)$ , although the effect for curl is more pronounced. This points toward a saturation effect similar to the saturation effect seen in the tensile index.

Performing the same type of comparison for Trial 4 (High-High), we see even stronger effects, especially for the second stage (Figure 13). The peaks in the first refining stage,

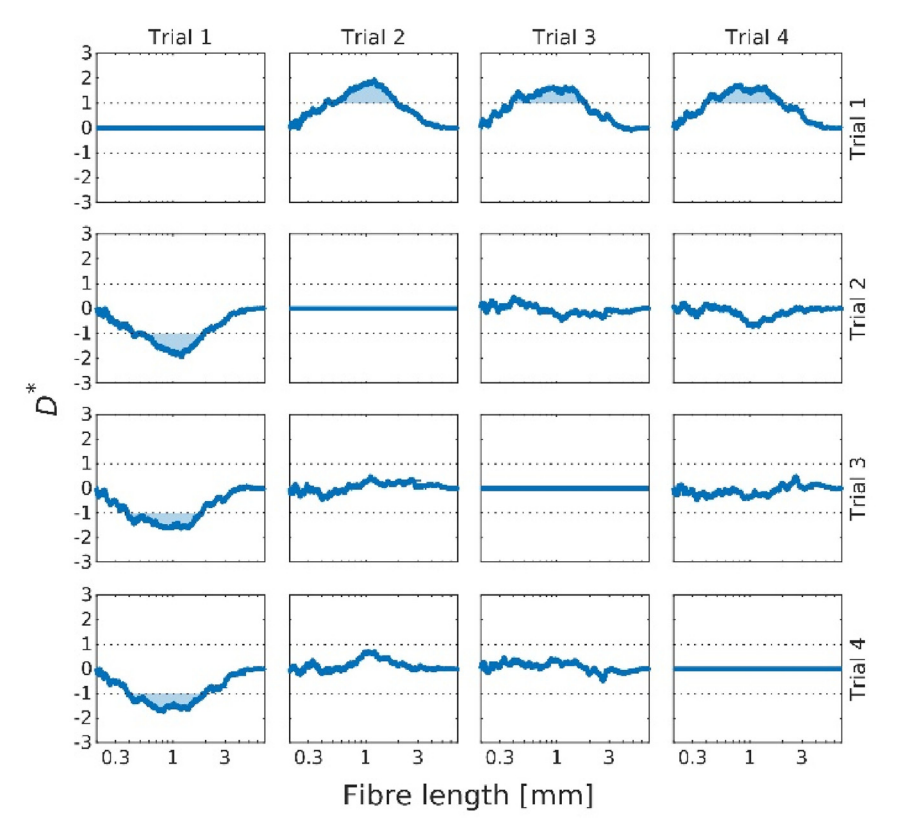


Figure 11: The length distribution of the LC refiner feed pulp in each trial compared with the other trials using KS statistics without Bonferroni correction. Since the peaks of Trial 1 exceed the absolute value 1, the feed pulp of Trial 1 is significantly different from the feed in the other trials.

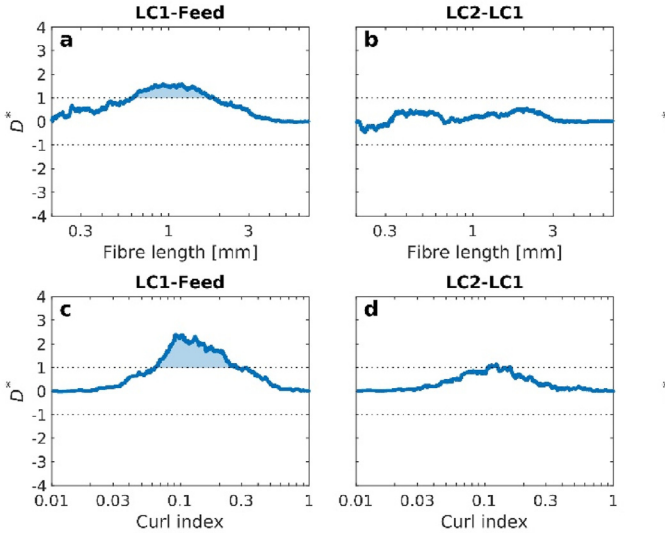
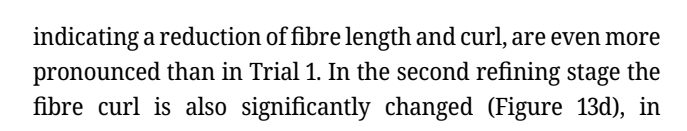


Figure 12: Pulp distribution changes across LC stages in Trial 1 (Low-Low) as quantified by D\*. The impact on fibre length across (a) the first LC stage, and (b) the second LC stage. Also, the impact on fibre curl across (c) the first LC stage, and (d) the second LC stage.



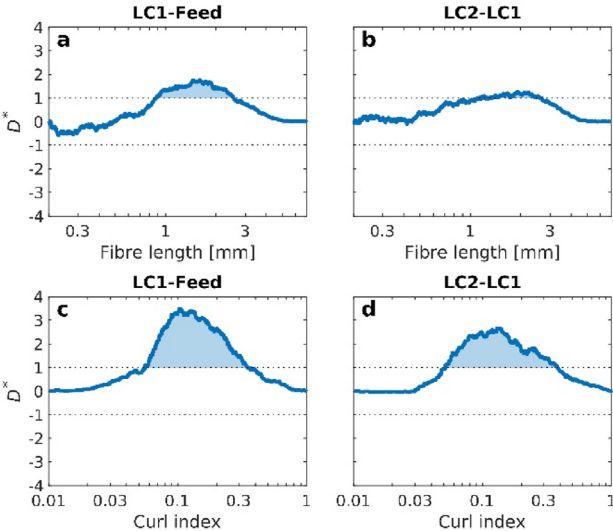


Figure 13: Pulp distribution changes across LC stages in Trial 4 (High-High) as quantified by D\*. The impact on fibre length across (a) the first LC stage, and (b) the second LC stage. Also, the impact on fibre curl across (c) the first LC stage, and (d) the second LC stage.

contrast to the corresponding results for Trial 1 (Figure 12d). The influence of using a higher SRE is thus clearly visualized with the KS-distribution.

#### 4.3 Distribution analysis

As a complement to the KS-analysis, the fibre data were also evaluated using distribution analysis. Two-dimensional (2D) distributions, such as curl versus fibre length, were generated by dividing the 2D domain into  $25 \times 25$  bins, with a logarithmic scale for fibre length and a linear scale for curl. Each fibre was assigned to a corresponding bin, producing a 2D histogram. To enable more effective comparisons, the distributions were normalized to a fixed number of fibres (here 50,000) and smoothed using kernel density functions, resulting in a less noisy dataset. A typical 2D distribution for curl versus fibre length is shown in Figure 14.

A 2D distribution plot can also be used to visualize the changes imposed by an LC stage, as exemplified in Figure 15, which shows the change in curl versus fibre length distributions over each one of the two refining stages in Trial 1 (Low-Low). When comparing the effects of LC1 and LC2 in distribution analyses across the four trials, the trends are similar to the observations in the KS-analysis. For instance, the peak in curl index in Figure 12c and d appear around Curl = 0.1, which corresponds to the approximate vertical position where the change in curl index shifts from positive (red) to negative (blue) values in Figure 15a and b.

Moreover, in Figure 15, both refining steps show qualitatively the same behaviour (LC1 in Figure 15a and LC2 in Figure 15b). A clear reduction of long fibres (2-4 mm) is observed, while the number of shorter fibres (0.3-2 mm) increases. The amount of short (0.1-0.2 mm) and curved fibres decreases, whereas the number of short, straight fibres rises. This reduction in curvature can be partly

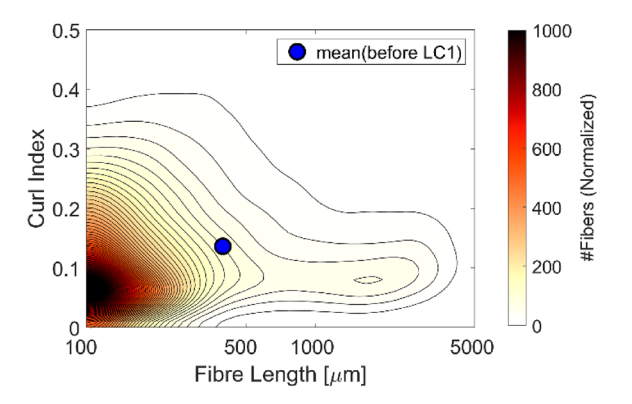


Figure 14: Two-dimensional distribution for curl versus logarithmic fibre length, using data for Trial 1 (Low-Low) before LC1. This data is normalized to 50,000 fibres. The interspacing between contour-lines is 20 fibres.

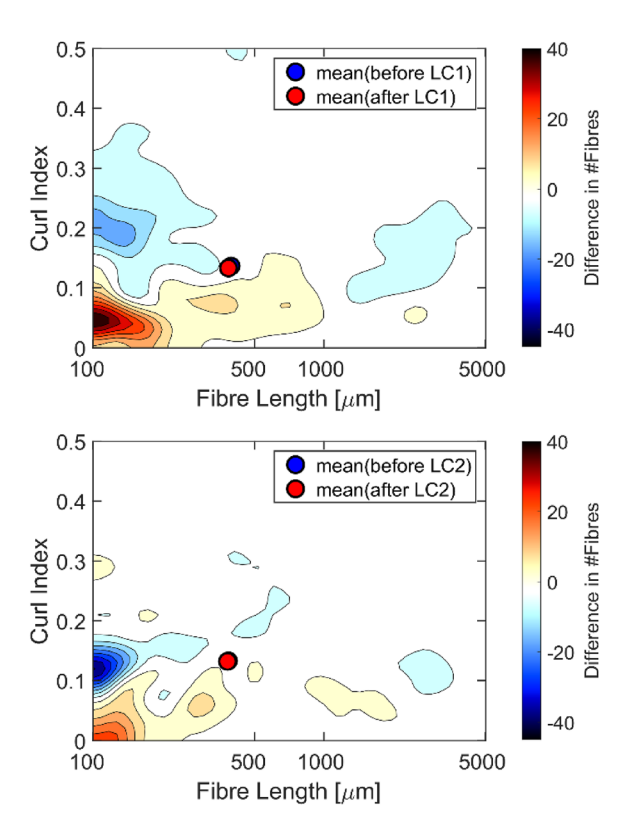


Figure 15: Differences between two-dimensional curl versus fibre length distributions, using data for Trial 1 (Low-Low). (a) LC1. (b) LC2. This data is normalized to 50,000 fibres. Blue and red colours in the surf plot indicate decrease and increase, respectively. The interspacing between contourlines is 5 fibres.

attributed to the geometric effect that naturally occurs when cutting a curved line into smaller segments.

Both the distribution analysis and the KS-statistics demonstrates that curl as well as fibre length decrease with refining, although the two methods have different strengths. For instance, distribution analysis illustrates (in 2D) where changes occur, while KS-statistics can determine whether these changes are statistically significant. By combining both methods, a deeper understanding of how to evaluate subtle differences in fibre distributions can be achieved. Note also that the difference in average values is very small (Figure 15a and b), so much more insight is gained by utilizing distributions.

# 5 Discussion

This study shows that the changes in pulp properties across the two refining stages differ. The refiners were equipped with different segment designs with considerably coarser

segments in the first refiner. This is a strategy from the mill to avoid plugging of the refiner segments with coarse start/ stop-pulp from the preceding HC refiners. The resulting 56 % higher intensity, calculated as specific edge load (Table 1) at a given motor load for the primary refiner, ought to influence the pulp properties development, especially the fibre length reduction, as has been reported in earlier work (e.g. Luukkonen et al. 2010). Despite the large difference in specific edge load, the fibre length reduction for the two stages were relatively similar.

However, the change in fibre length over the two refining stages depends on how fibre length is analysed. The change, based on length-length-weighted average, is similar for the two refining stages, whereas the unweighted distributions analysed with KS-statistics indicates somewhat larger changes in the primary stage. Thus, this investigation shows that analysing fibre distributions can reveal changes that are not clearly seen when averages are studied.

The split of applied energy (Low-High compared to High-Low) resulted in similar pulp property development. In our trial the difference between Low and High was relatively small (around 20 kWh/bdt) since we wanted to keep the conditions within the span of normal operation. Larger differences, which will be considered in future trials, could result in other conclusions.

Our KS-analysis revealed that each LC refining stage induces a statistically significant change in the fibre curl distribution, characterized by a shift to lower values of curl, which is most pronounced in the primary stage. By visual inspection, the shape of the  $D_{AB}^*(C)$  curves are consistent, but with different magnitude (Figures 12c and d and 13c and d). Thus, the same particle fractions are affected, but to a different extent depending on refining stage and SRE. The lower tensile index increase across the second stage might be associated with the lower reduction in curl, since the curl often influences the tensile index (Ferritsius et al. 2024). Moreover, a higher specific energy yields a larger reduction in curl. A similar trend was noted in the length distribution of fibres, albeit with lesser statistical significance. Other strength-related properties, such as burst index (Figure 6), did not show a similar trend as tensile index (Figure 3).

The KS-analysis thus revealed a larger impact of the first refining step on the fibre distributions, in agreement with corresponding experimental observations for the tensile index. However, it is not yet fully understood why the tensile index is the only investigated strength-related property which shows a smaller change across the second refining stage. One possible explanation is that the tensile index is more strongly influenced by fibre curl compared to, for example, burst index.

#### 6 Conclusions

Our study highlights the higher refining efficiency of the primary LC refiner stage in terms of tensile index increment per applied specific energy, indicating a saturation effect as additional energy is applied in the second stage. Using KS statistics, we demonstrated that the first LC stage leads to a greater reduction in fibre length and curl index compared to the second refining stage, with particularly strong significance observed for the curl index. The saturation effect seen in the tensile index is statistically linked to a reduction in curl index.

The most beneficial mode of operation, in terms of fibre length at given tensile index, was to apply low specific energy in both stages. The energy split between the two stages (Low-High or High-Low) did not result in a significant difference in pulp properties development.

By identifying the saturation effect in tensile index, and a presumptive connection to fibre curl, we contribute to a more comprehensive understanding of LC refining of mechanical pulp as well as its limitations and potential for increased energy efficiency.

**Acknowledgments:** The authors thank Holmen for support in facilitating mill trials and experimentation.

Research ethics: Not applicable.

Author contributions: The authors have accepted responsibility for the entire content of this manuscript and approved its submission.

**Informed consent:** Not applicable.

Use of Large Language Models, AI and Machine Learning

Tools: None declared.

Conflict of interest: The authors state no conflict of interest. Research funding: The work has been carried out within the Strategic Innovation Program for Process Industrial IT and Automation, a joint initiative by Vinnova, Formas, and the Swedish Energy Agency, as Vinnova grant agreement No. 2022-03597. The work was done within the research profile Neopulp financed by the Knowledge foundation. S. B. Lindström thanks Svenska Cellulosa AB (SCA) for financial support.

Data availability: The raw data can be obtained on request from the corresponding author.

# **Appendix**

Table A1: Data for the four trials.

Property		Trial 1 Low-Low		Trial 2 High-Low			Trial 3 Low-High			Trial 4 High-High			
SRE acc.	kWh/bdt	0	84	166	0	105	190	0	85	186	0	103	204
CSF	ml	196	172	153	184	154	141	182	159	139	183	154	132
PulpEye													
Shive weight %	%	0.25	0.32	0.22	0.33	0.27	0.16	0.29	0.27	0.17	0.36	0.23	0.19
Shive sum	N <u>o</u> /g	637	802	706	734	686	586	724	737	618	870	728	649
Fibre length <sup>a</sup>	mm	1.87	1.85	1.79	1.89	1.76	1.77	1.85	1.8	1.73	1.89	1.84	1.72
FiberTester													
Fibre length <sup>a</sup>	mm	1.74	1.7	1.67	1.69	1.63	1.62	1.72	1.67	1.63	1.7	1.64	1.58
Fibre length <sup>b</sup>	mm	2.67	2.66	2.63	2.64	2.57	2.52	2.69	2.62	2.55	2.64	2.56	2.48
60 g/m <sup>2</sup> sheets													
Density 60 g sheet	kg/m³	250	260	272	258	270	276	259	281	294	249	268	292
Tensile index	Nm/g	33.1	35.8	41.4	33.8	39.5	41.8	36.2	40.2	41.8	35.1	39.7	41.6
Stretch at break	%	2.43	2.5	2.56	2.47	2.57	2.39	2.41	2.38	2.47	2.43	2.53	2.49
Tensile stiffness	kN/m	203	214	245	209	245	265	218	249	257	211	241	259
Burst index	%	2.05	2.23	2.46	2.11	2.24	2.35	2.09	2.39	2.46	2.18	2.41	2.55
120 g/m² sheets													
Density 120 g sheet	kg/m³	285	310	344	294	318	327	297	340	365	299	322	366
SCT index	Nm/g	11.3	12.4	15.4	11.3	13.2	14.4	11.5	14.8	16.5	12.2	13.2	17

<sup>&</sup>lt;sup>a</sup>Length-weighted average. <sup>b</sup>Length-length-weighted average.

# References

- Anderson, T.W. and Darling, D.A. (1952). Asymptotic theory of certain "goodness of fit" criteria based on stochastic processes. Ann. Math. Stat. 23: 193-212, https://doi.org/10.1214/aoms/1177729437.
- Andersson, S., Sandberg, C., and Engstrand, P. (2012), Comparison of mechanical pulps from two stage HC single disc and HC double disc -LC refining. Appita J. 65: 57-62.
- Cramer, H. (1928). On the composition of elementary errors. Scand. Actuar. J. 1928: 13-74, https://doi.org/10.1080/03461238.1928.10416862.
- Fernando, D., Gorski, D., Sabourin, M., and Daniel, G. (2013). Characterization of fiber development in high- and low-consistency refining of primary mechanical pulp. Holzforschung 67: 735-745, https://doi.org/10.1515/hf-2012-0135.
- Ferritsius, R., Reyier Österling, S., and Ferritsius, O. (2012). Development of fibers in LC- and HC- refining. Nord. Pulp Pap. Res. J. 27: 860-871, https://doi.org/10.3183/npprj-2012-27-05-p860-871.
- Ferritsius, R., Sandberg, C., Ferritsius, O., Rundlöf, M., Daniel, G., Mörseburg, K., and Fernando, D. (2020). Development of fibre properties in mill scale high- and low consistency refining of thermomechanical pulp (part 1). Nord. Pulp Pap. Res. J. 35: 589-599, https://doi.org/10.1515/npprj-2020-0027.

- Ferritsius, R., Sandberg, C., Rundlöf, M., Ferritsius, O., Daniel, G., Engberg, B.A., and Nilsson, F. (2024). Development of fibre properties in mill scale: high- and low consistency refining of thermomechanical pulp (part 2) - importance of fibre curl. Nord. Pulp Pap. Res. J. 39: 575-585, https://doi.org/10.1515/npprj-2024-0049.
- Gorski, D., Luukkonen, A., Sabourin, M., and Olson, J. (2012). Two-stage low-consistency refining of mechanical pulp. Appita J. 65: 244-249.
- Guangdong, Y., Xu, E.C., Jozic, D., and Fitz, M. (2011). P-RC APMP lines at SUN paper group. In: Int. mech. pulping conf., Xian, China, pp. 165-169.
- Hill, J., Johansson, L., and Mörsburg, K. (2017). ATMP pulping of Norway spruce - pulp property development and energy efficiency. Nord. Pulp Pap. Res. J. 32: 70-86.
- Kolmogorov, A.N. (1933). Sulla determinizione empirica di una legge di distribuzione. In: Giorn. ist. ital. attuari, pp. 83-91.
- Kuiper, N.H. (1960). Tests concerning random points on a circle. *Indagat*. Math. 63: 38-47, https://doi.org/10.1016/s1385-7258(60)50006-0.
- Luukkonen, A., Olson, J.A., and Martinez, D.M. (2010). Low consistency refining of mechanical pulp, effect of gap, speed and power. JPPS 36: 28-34.
- Von Mises, R. (1928). Wahrscheinlichkeit Statistik und Wahrheit, 1st ed Springer-Verlag Berlin, Vienna.

- Marsaglia, G., Tsang, W.W., and Wang, J. (2003). Evaluating Kolmogorov's distribution. J. Stat. Software 8: 1-4, https://doi.org/10.18637/jss.v008. i18.
- de Montmorency, W.H. (1958). Refining low-energy, high-production groundwood with a double-disc refiner. Pulp Pap. Mag. Can. 59: 203–223.
- Musselman, R.L., Letarte, D., and Simard, R. (1997). Third stage low consistency refining of TMP for energy savings and quality enhancement. In: PIRA 4th int. refining conf., Fiuggi.
- Page, D.H., Seth, R.S., Jordan, B.D., and Barbe, M.C. (1985). Curl, crimps, kinks and microcompressions in pulp fibres - their origin, measurement, and significance. In: Punton, V. (Ed.). Papermaking raw materials, trans. of the VIIIth fund. res. symp., Oxford, pp. 183-227.
- Peng, F., Xing, J., Olsson, G., Nåvik, J., and Granfeldt, T. (2018) High quality eucalyptus CTMP for board grades at Stora Enso Beihai mill. In: Int. mech. pulping conf., Trondheim, Norway, Session 7(2).

- Sabourin, M. (2007). Minimizing TMP energy consumption using a combination of chip pre-treatment, RTS and multiple stage low consistency refining. In: Int. mech. pulping conf., Minneapolis.
- Sandberg, C., Berg, J.-E., and Engstrand, P. (2017). Low consistency refining of mechanical pulp - system design. TAPPI J. 16: 419-429, https://doi. org/10.32964/tj16.7.419.
- Sandberg, C., Ferritsius, O., and Ferritsius, R. (2021). Energy efficiency in mechanical pulping - definitions and considerations. Nord. Pulp Pap. Res. J. 36: 425-434, https://doi.org/10.1515/npprj-2021-0013.
- Smirnov, N.V. (1944). Approximate distribution laws for random variables, constructed from empirical data. Uspekhi Mat. Nauk 10: 179-206.
- Stephens, M.A. (1970). Use of the Kolmogorov-Smirnov, Cramer-von Mises and related statistics without extensive tables. I. Roy. Stat. Soc. B 32: 115-122, https://doi.org/10.1111/j.2517-6161.1970.tb00821.x.